THE JOURNAL OF PROSTHETIC DENTISTRY

RESEARCH AND EDUCATION

Scan accuracy and time efficiency of different implant-supported fixed partial denture situations depending on the intraoral scanner and scanned area: An in vitro study

Mustafa Borga Donmez, DDS, PhD,[a] Ayse Mathey, Dr Med Dent,[b] Fabio Gäumann, Med Dent,[c] Amber Mathey, Med Dent,[d] Burak Yilmaz, DDS, PhD,[e] and Samir Abou-Ayash, Prof Dr Med Dent[f]

ABSTRACT

Statement of problem. The type of intraoral scanner (IOS), region of the implant, and extent of the scanned area have been reported to affect scan accuracy. However, knowledge of the accuracy of IOSs is scarce when digitizing different partially edentulous situations either with complete- or partial-arch scans.

Purpose. The purpose of this in vitro study was to investigate the scan accuracy and time efficiency of complete- and partial-arch scans of different partially edentulous situations with 2 implants and 2 different IOSs.

Material and methods. Three maxillary models with implant spaces at the lateral incisor sites (anterior 4-unit), right first premolar and right first molar sites (posterior 3-unit), or right canine and right first molar sites (posterior 4-unit) were fabricated. After placing implants (Straumann S RN) and scan bodies (CARES Mono Scanbody), models were digitized by using an optical scanner (ATOS Capsule 200MV120) to generate reference standard tessellation language (STL) files. Complete- or partial-arch scans (test scans) of each model were then performed by using 2 IOSs (Primescan [PS] and TRIOS 3 [T3]) (n=14). The duration of the scans and the time needed to postprocess the STL file until the design could be started were also recorded. A metrology-grade analysis software program (GOM Inspect 2018) was used to superimpose test scan STLs over the reference STL to calculate 3D distance, interimplant distance, and angular (mesiodistal and buccopalatal) deviations. Nonparametric 2-way analysis of variance followed by Mann-Whitney tests with Holm correction were used for trueness, precision, and time efficiency analyses (α=.05).

Results. The interaction between IOSs and scanned area only affected the precision of the scans when angular deviation data were considered ($P \leq .002$). Trueness of the scans was affected by IOSs when 3D distance, interimplant distance, and mesiodistal angular deviations were considered. The scanned area affected only 3D distance deviations ($P \leq .006$). IOSs and scanned area significantly affected the precision of scans when 3D distance, interimplant distance, and mesiodistal angular deviations were considered, while only IOSs significantly affected buccopalatal angular deviations ($P \leq .040$). Scans from PS had higher accuracy when 3D distance deviations were considered for the anterior 4-unit and posterior 3-unit models ($P \leq .030$), when interimplant distance deviations were considered for complete-arch scans of the posterior 3-unit model ($P \leq .048$), and when mesiodistal angular deviations were considered in the posterior 3-unit model ($P \leq .050$). Partial-arch scans had higher accuracy when 3D distance deviations of the posterior 3-unit model were considered ($P \leq .002$). PS had higher time efficiency regardless of the model and scanned area ($P \leq .010$), while partial-arch scans had higher time efficiency when scanning the posterior 3-unit and posterior 4-unit models with PS and the posterior 3-unit model with T3 ($P \leq .050$).

Conclusions. Partial-arch scans with PS had similar or better accuracy and time efficiency than other tested scanned area-scanner pairs in tested partial edentulism situations. (J Prosthet Dent 2023;■:■-■)

Funding: Supported by the German Association of Oral Implantology (DGI). The funds were used for the acquisition of study materials and for the statistical analyses. The funders were not involved in any further aspect of this study.

[a]Assistant Professor, Department of Prosthodontics, Faculty of Dentistry, Istinye University, İstanbul, Turkey; Visiting Researcher, Department of Reconstructive Dentistry and Gerodontology, School of Dental Medicine, University of Bern, Bern, Switzerland.
[b]Senior Lecturer, Department of Reconstructive Dentistry and Gerodontology, School of Dental Medicine, University of Bern, Bern, Switzerland.
[c]Doctoral Candidate, Department of Reconstructive Dentistry and Gerodontology, School of Dental Medicine, University of Bern, Bern, Switzerland.
[d]Doctoral Candidate, Department of Reconstructive Dentistry and Gerodontology, School of Dental Medicine, University of Bern, Bern, Switzerland.
[e]Associate Professor, Department of Reconstructive Dentistry and Gerodontology, University of Bern, Bern, Switzerland; Associate Professor, Department of Restorative, Preventive and Pediatric Dentistry, School of Dental Medicine, University of Bern, Bern, Switzerland; Adjunct Professor, Division of Restorative and Prosthetic Dentistry, The Ohio State University, Columbus, Ohio.
[f]Deputy Department Chair, Department of Reconstructive Dentistry and Gerodontology, University of Bern, Bern, Switzerland.

Clinical Implications

Scans of anterior and posterior 3- or 4-unit two-implant-supported fixed partial dentures may be more reliable and time efficient when partial arches are scanned by using PS.

Intraoral scanners (IOSs) and a direct digital workflow in which scan bodies are used to acquire the 3-dimensional (3D) position of the implant have been reported to minimize the shortcomings of conventional impressions.[1-8] Digital implant scans have the advantage of improved patient acceptance,[9,10] easier data transfer and communication,[11] direct visualization of the cast,[12] and time efficiency.[7,13] However, to be routinely used, digital scans should be as accurate as conventional impressions.[14] Inaccuracy may result in misfit, which could eventually lead to biological and mechanical problems that could jeopardize the success of implant-supported prostheses.[15-18]

Trueness (closeness of a measurement to the actual dimensions) and precision (closeness of repetitive measurements to each other) comprise accuracy.[19-21] The accuracy of IOSs has been a concern[22] and reported to depend on different factors,[14,23,24] including the IOS itself as IOSs use different image-acquisition methods and algorithms to reconstruct the data.[19] Another factor that may affect scan accuracy is the extent of the edentulous area,[25] as an increased span length has been reported to reduce scan accuracy.[3,13,15,16,26,27] The region of the scan (anterior or posterior) is another influential factor on which no consensus has yet been reached,[12,28] and performing a complete- or partial-arch scan may affect the scan accuracy depending on the region scanned.[29]

The authors are aware of a few studies that focused on the scan accuracy of implants placed for fixed partial dentures (FPDs),[3,13,16,30-33] but only 1 investigated the scan accuracy of anterior implants for an FPD.[33] In addition, those studies[3,13,16,30-33] did not involve the effect of the extent of the scanned area on accuracy or on the time efficiency of the scans performed. Therefore, the aim of the present study was to evaluate the scan accuracy and time efficiency of 2 different IOSs in 3 different FPD situations (2 implants placed at maxillary lateral incisor sites, maxillary right canine and first molar sites, or maxillary right first premolar and first molar sites) when either complete- or partial-arch scans were performed. In addition, the time required for performing scans and processing was compared. The null hypotheses were that the type of IOS and the scanned area would not affect the trueness or precision of implant scans in an FPD situation and that the type of IOS and the scanned area would not affect the scan and file transfer time efficiency in an FPD situation with 2 implants.

MATERIAL AND METHODS

A CAD software program (Zirkonzahn.Modellier; Zirkonzahn GmbH) was used to design 3 maxillary models simulating different FPD situations: a single anterior bilateral edentulous (Kennedy class IV) situation with 2 implants located at the right and left lateral incisor sites (anterior 4-unit), a unilateral distal extension situation (Kennedy class II) with 2 implants located at the right first premolar and right first molar sites (posterior 3-unit), and a unilateral distal extension situation (Kennedy class II) with 2 implants located at the right canine and right first molar sites (posterior 4-unit). Implant spaces with threads allowed the implants to be tightened 2 mm submucosally.[33] Cobalt-chromium-molybdenum alloy[34] (M5; Zirkonzahn GmbH) was used to mill the models, and tissue-level titanium implants (Straumann S RN 4.1×10 mm; Institut Straumann AG) were screwed and fixed with a metal adhesive (Adesso Split Justierkleber; Baumann Dental GmbH). Scan bodies (CARES Mono Scanbody; Institut Straumann AG) were tightened to the implants to 15 Ncm, and an antireflective scan spray (IP Scan Spray; IP-Division) was applied on each model. A reference standard tessellation language (STL) file of each model was generated with an industrial-grade optical scanner (ATOS Capsule 200MV120; GOM GmbH) and a software program (Pro 8.1; GOM GmbH) (Fig. 1).

After reference scans, a single operator (A.M.) digitized each model by using 2 different IOSs (Primescan; Dentsply Sirona [PS], and TRIOS 3; 3Shape [T3]) installed with the most recent versions of their software programs. The number of scans performed by each IOS was determined according to Welch tests based on the results of previous studies (α=.05 and 1-β=above 80%)[9,35] that deemed 14 scans sufficient. Thus, a total of 168 scans were performed given that both complete- and partial-arch scans were performed for each model. The IOSs were calibrated according to their manufacturers' recommendations before each set of scans. The choice of which IOS to begin with was made with a coin toss that resulted in PS. The operator took 5-minute breaks between each set of scans to minimize fatigue-related inaccuracies[6] and the risk of bias. For each model, the partial-arch scan was performed first, followed by the complete-arch scan until all scans were completed. Each model had been mounted to phantom heads with face masks by using 2-sided adhesive tape, and its surface was sprayed with the same antireflective spray. To ensure a standardized layer thickness, model surfaces were not contacted until all scans were performed. An opposing dentate model was also mounted. Regardless of the IOS, partial-arch scans of the anterior 4-unit model involved the area between the right first premolar and the left first premolar, while partial-arch scans of the posterior 3-unit and posterior 4-unit models involved the area between

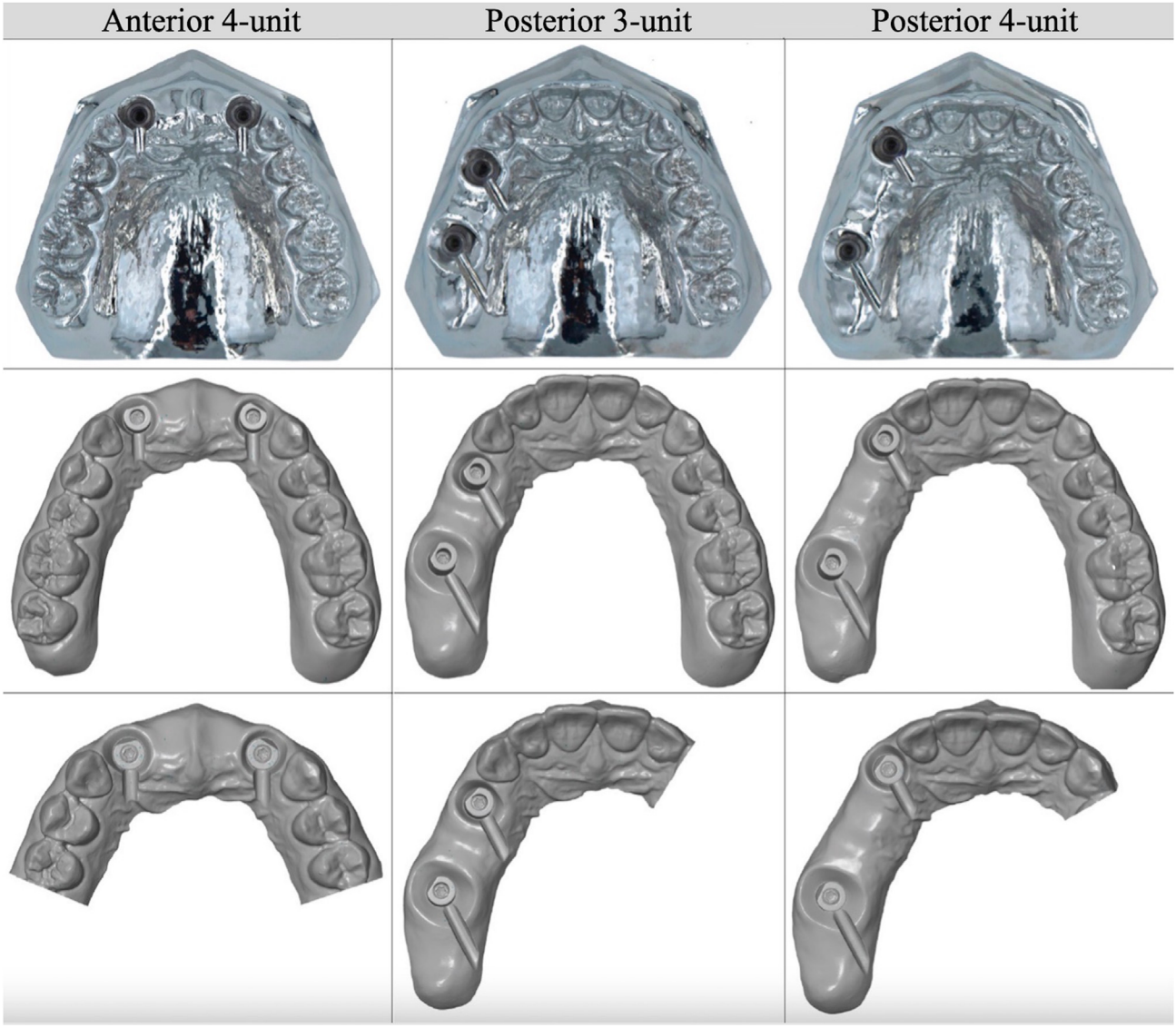

Figure 1. Master models and reference scan of each model.

the right second molar and midline. For complete-arch scans, the recommended scan pattern of each IOS (starting from the lingual surfaces and then the occlusal and buccal surfaces for PS; starting from the occlusal surfaces and then the lingual and buccal surfaces for T3)[19] was used. All scans were performed in the same room (23 °C, 1000 lux illuminance),[36] exported in STL format, and imported into a CAD software program (Zirkonzahn.Modellier; Zirkonzahn GmbH). The time needed for scans, data processing, exporting data from the IOS, importing data into the CAD software program, and data processing in the CAD software program until the design could be started was recorded with a stopwatch (Rotilabo; Carl Roth GmbH).

The STL files were trimmed approximately 2 mm apical to the gingival zenith of the remaining teeth with a software program (Meshmixer v3.5.474; Autodesk Inc) for standardization and imported into a metrology-grade 3D analysis software program (GOM Inspect 2018; GOM GmbH) for accuracy analyses. Automatic prealignment and global best fit excluding only the scan body surface data were used to superimpose the complete-arch scan STL files over the reference scan STL (Fig. 2). The same methodology program was used for partial-arch scans after selecting the area of superimposition according to the IOS scan.[1] After superimposition, 8 points were defined on each scan body of the reference scan, and their coordinates were recorded; this allowed a standardized selection of points throughout the analyses. The points were projected onto the IOS scan, and 3D distance deviations at these points were automatically calculated. The interimplant distance deviation was calculated by measuring the distance between 2 of the previously defined points (1 on each scan body) for reference and

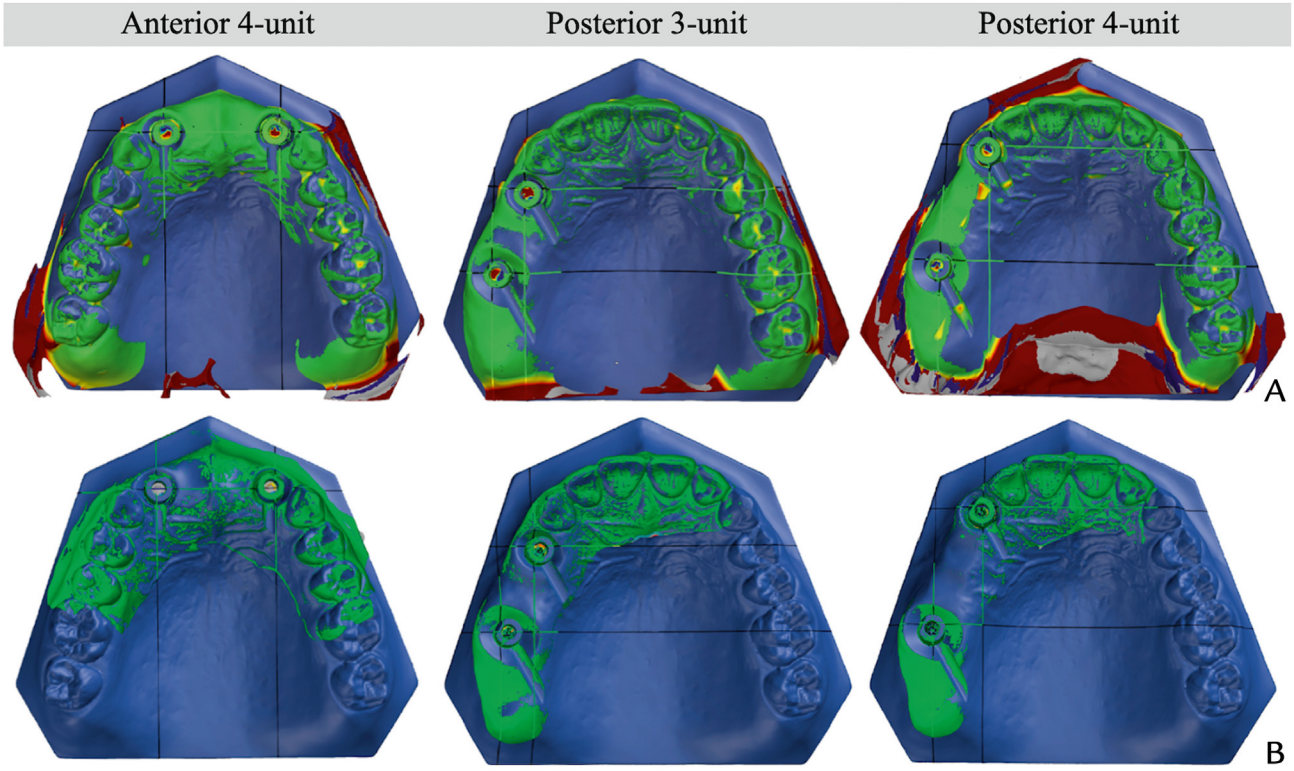

Figure 2. Color maps generated by superimpositions and planes used for angular deviation analyses. A, Complete-arch scans. B, Partial-arch scans.

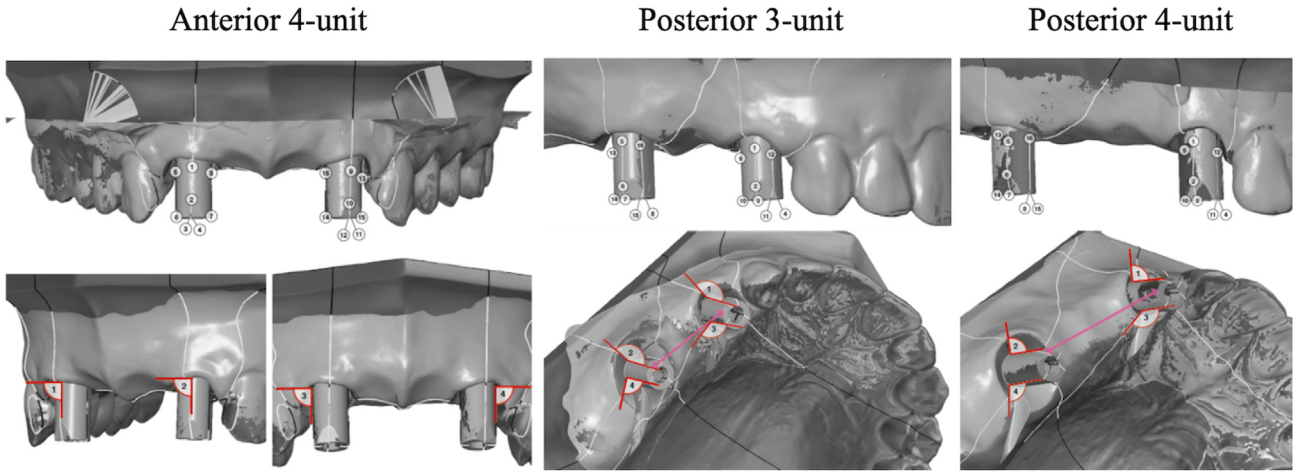

Figure 3. Overview of points 1-16 (upper images) and angles (lower images) used for accuracy analyses. Analyses of buccopalatal angular deviations performed by using angles 1 and 2, while analyses of mesiodistal angular deviations performed by using angles 3 and 4. *Red* vectors demonstrate interimplant distances.

IOS scans. In addition, 2 vectors (1 in mesiodistal and 1 in buccopalatal direction) passing through 2 points on each scan body were generated. These vectors were used to calculate the mesiodistal and buccopalatal angular deviations between the reference and IOS scans (Fig. 3).[33]

Group data of some of the parameters evaluated were skewed, which led to the rejection of normality, and nonparametric analyses were used. Median values and interquartile ranges for 3D distance, interimplant distance, and angular deviations (mesiodistal and buccopalatal) were calculated for trueness (distance between test and reference scans) and precision (variance between scans) analyses. Median working times and their interquartile ranges were also calculated. Data were evaluated by using nonparametric 2-way analysis of variance tests,

Table 1. Median and interquartile range (25% to 75%) values of measured deviations (trueness) for each scanner-scanned area pair in each model

			Distance Deviations (μm)		Angular Deviations (Degrees)	
Model	**Scanned Area**	**Scanner**	**3D**	**Interimplant**	**Mesiodistal**	**Buccopalatal**
Anterior 4-unit	Complete arch	PS	155.94^{aA} (142.40-158.88)	20.15^{aA} (8-39.28)	0.23^{aA} (0.11-0.34)	0.33^{aA} (0.28-0.40)
		T3	163.48^{bA} (159.87-174.32)	11.50^{aA} (4.14-34.44)	0.21^{aA} (0.13-0.34)	0.21^{aA} (0.12-0.29)
	Partial arch	PS	155.53^{aA} (152.04-162.66)	15.57^{aA} (6.41-22.6)	0.17^{aA} (0.11-0.34)	0.27^{aA} (0.11-0.38)
		T3	172.17^{bA} (169.39-180.69)	8^{aA} (2.25-24.53)	0.27^{aA} (0.20-0.60)	0.14^{aA} (0.04-0.38)
Posterior 3-unit	Complete arch	PS	13.66^{aB} (12.24-17.87)	2.04^{aA} (1.07-3.32)	0.06^{aA} (0.04-0.09)	0.04^{aA} (0.03-0.06)
		T3	32.05^{bB} (28.35-34.34)	3.86^{bA} (2.98-6.24)	0.08^{bA} (0.07-0.16)	0.06^{aA} (0.04-0.10)
	Partial arch	PS	8.75^{aA} (6.97-10)	1.27^{aA} (1-2.81)	0.04^{aA} (0.03-0.06)	0.06^{aA} (0.04-0.09)
		T3	22.81^{bA} (18.91-25.35)	3.14^{aA} (1.32-4.75)	0.10^{bA} (0.07-0.20)	0.06^{aA} (0.04-0.08)
Posterior 4-unit	Complete arch	PS	127.03^{aA} (108.99-141.07)	20.58^{aA} (1.86-36.17)	0.58^{aA} (0.36-0.8)	0.11^{aA} (0.06-0.52)
		T3	111.66^{aA} (107.23-144.06)	21.84^{aA} (5.34-36.4)	0.37^{aA} (0.18-0.96)	0.21^{aA} (0.11-0.58)
	Partial arch	PS	119.42^{aA} (99.42-136.56)	24.94^{aA} (2.08-36.95)	0.32^{aA} (0.22-0.46)	0.34^{aA} (0.05-0.61)
		T3	112.15^{aA} (99.4-148.75)	20.78^{aA} (1.45-36.27)	0.56^{aA} (0.29-0.70)	0.09^{aA} (0.04-0.46)

PS, Primescan; T3, TRIOS 3. Different superscript lowercase letters in each column indicate significant differences between scanners for each model-scanned area pair. Different superscript uppercase letters indicate significant differences between scanned areas for each model-scanner pair ($P<.05$).

which included IOS and scanned area as the main factors and their interaction. Significant effects were further resolved by using exact Mann-Whitney tests with Holm correction. All analyses were performed with a software program (R v4.0.2; The R Foundation) ($\alpha=.05$).

RESULTS

When 3D distance deviations were considered, significant differences between scanners were observed for the anterior 4-unit and posterior 3-unit models, while significant differences between scanned areas were observed for the posterior 3-unit model ($P<.001$). PS had lower deviations than T3 for both models regardless of the scanned area ($P\leq.030$). In addition, partial-arch scans resulted in lower deviations than complete-arch scans of the posterior 3-unit model for both scanners ($P\leq.002$). When interimplant distance deviations were considered, significant differences between scanners were observed only in the posterior 3-unit model ($P=.006$), as PS had lower deviations than T3 when complete-arch scans were considered ($P=.048$). When mesiodistal angular deviations were considered, significant differences between scanners were observed only for the posterior 3-unit model ($P<.001$), as PS had lower deviations than T3, regardless of the scanned area ($P\leq.05$). When buccopalatal angular deviations were considered, no significant differences were observed between different scanners and scanned areas ($P\geq.06$). Table 1 summarizes the descriptive statistics of deviation values within each model for each scanner-scanned area pair, while Figure 4 shows the box-plot graph of measured deviations.

When 3D distance deviations were considered, scanners affected the precision of the scans in all models ($P<.001$), and scanned area affected the precision of the scans of the anterior 4-unit and posterior 3-unit models ($P<.001$). Regardless of the model, PS and partial-arch scans had higher precision ($P\leq.002$). When interimplant distance deviations were considered, scanners affected the precision of the scans of the anterior 4-unit and posterior 3-unit models ($P\leq.040$), and scanned area affected the precision of the scans of the anterior 4-unit model ($P<.001$). However, Mann-Whitney U tests revealed higher precision for PS of the posterior 3-unit model ($P<.001$) and for partial-arch scans of the anterior 4-unit model when PS was used ($P=.005$). When mesiodistal angular deviations were considered, the interaction between the scanner type and the scanned area affected the precision of scans of the posterior 3-unit model ($P<.001$), while both scanner and scanned area affected the precision of scans of the posterior 4-unit model ($P<.001$). In the posterior 3-unit model, PS had higher precision than T3 regardless of the scanned area ($P\leq.010$), while complete-arch scans had higher precision when T3 was used ($P<.001$). In the posterior 4-unit model, PS had higher precision than T3 when partial-arch scans were performed ($P=.002$), and partial-arch scans had higher precision than complete-arch scans when PS was used ($P=.003$). When buccopalatal angular deviations were considered, the interaction between the scanner type and the scanned area affected the precision of the scans in the posterior 3-unit and posterior 4-unit models ($P\leq.002$), while scanner type affected the precision of scans of the anterior 4-unit model ($P=.009$). However, the Mann-Whitney U test showed nonsignificant differences between scanners of the anterior 4-unit model regardless of the scanned area ($P=.060$). In the posterior 3-unit model, PS had higher precision than T3 when complete-arch scans were performed ($P<.001$). In the posterior 4-unit model, T3 had higher precision than PS when partial-arch scans were performed ($P=.040$), and partial-arch scans had higher precision when T3 was used ($P=.020$). Table 2 summarizes the descriptive statistics of precision of deviation values in each model for

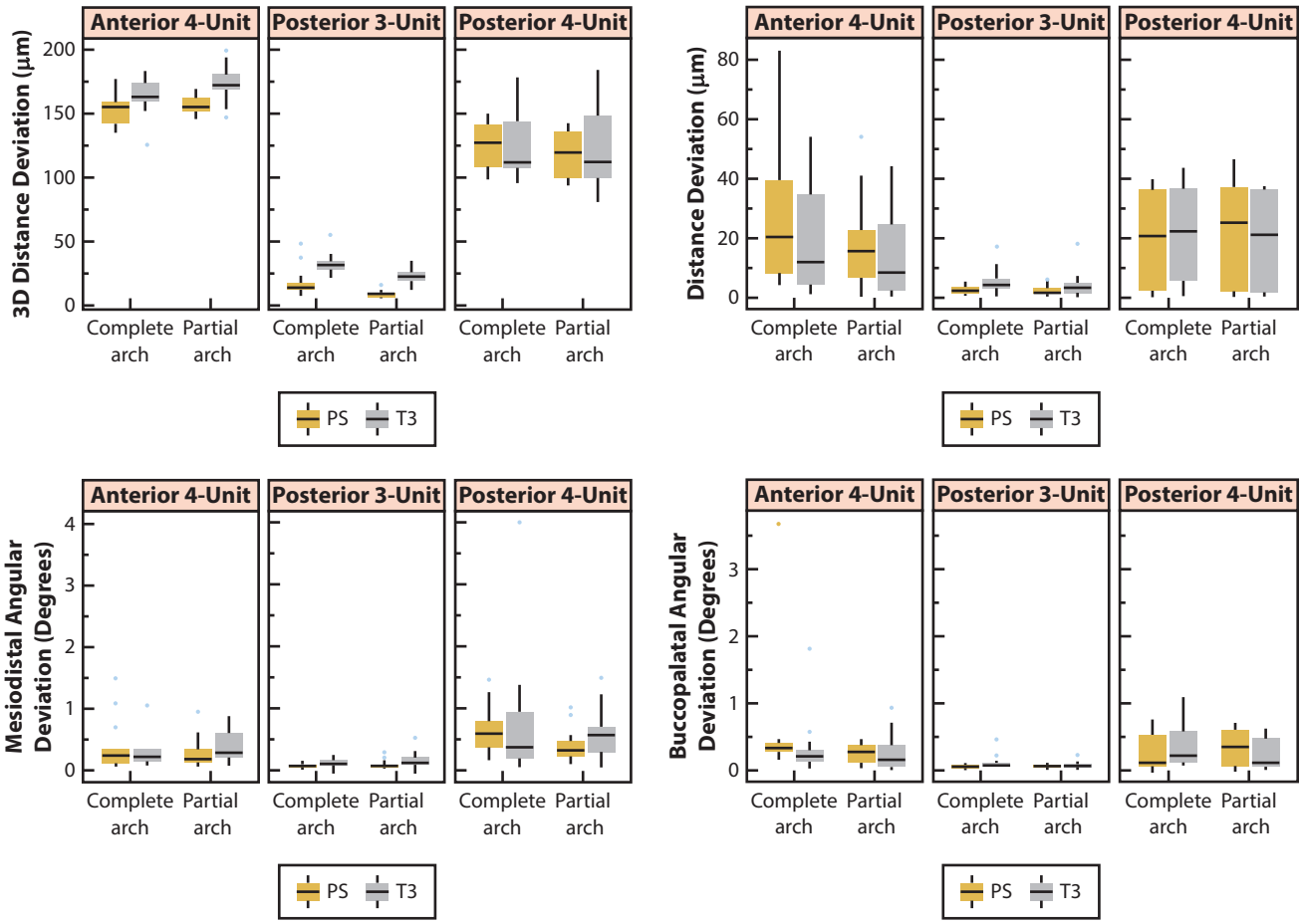

Figure 4. Box-plot graphs of measured deviations for each scanner-scanned area pair in each model. PS, Primescan; T3, TRIOS 3.

Table 2. Median and interquartile range (25% to 75%) values of precision of scans for each scanner-scanned area pair within each model

			Distance Deviations (μm)		Angular Deviations (Degrees)	
Model	**Scanned Area**	**Scanner**	**3D**	**Interimplant**	**Mesiodistal**	**Buccopalatal**
Anterior 4-unit	Complete arch	PS	35.21^{aB} (29.14-43.87)	21.06^{aB} (10.45-45.85)	0.21^{aA} (0.11-0.67)	0.12^{aA} (0.06-0.23)
		T3	57.21^{bB} (46.71-86.37)	15.08^{aA} (6.45-35.98)	0.16^{aA} (0.07-0.71)	0.16^{aA} (0.10-0.33)
	Partial arch	PS	27.84^{aA} (23.59-30.9)	13.62^{aA} (6.74-21.87)	0.16^{aA} (0.06-0.33)	0.17^{aA} (0.08-0.28)
		T3	49.87^{bA} (43.98-58.3)	14^{aA} (5.33-25.64)	0.23^{aA} (0.1-0.49)	0.23^{aA} (0.07-0.38)
Posterior 3-unit	Complete arch	PS	9.18^{aB} (7.06-24.08)	1.54^{aA} (0.80-2.39)	0.04^{aA} (0.02-0.06)	0.03^{aA} (0.01-0.04)
		T3	21.79^{bB} (13.9-31.36)	3^{bA} (1.11-6.32)	0.06^{bA} (0.03-0.11)	0.04^{bA} (0.01-0.12)
	Partial arch	PS	7.48^{aA} (6.18-9.46)	1.27^{aA} (0.44-4)	0.03^{aA} (0.01-0.12)	0.04^{aA} (0.01-0.05)
		T3	16.25^{bA} (12.5-19.38)	2.77^{bA} (1.23-4.93)	0.10^{bB} (0.05-0.20)	0.04^{aA} (0.01-0.06)
Posterior 4-unit	Complete arch	PS	47.79^{aA} (33.13-59.41)	29.34^{aA} (1.6-34.62)	0.37^{aB} (0.18-0.68)	0.40^{aA} (0.06-0.49)
		T3	69.32^{bA} (50.38-79.28)	28.30^{aA} (2.54-31.68)	0.44^{aA} (0.16-1.03)	0.38^{aB} (0.09-0.8)
	Partial arch	PS	55.71^{aA} (27.55-66.48)	23.43^{aA} (1.75-35.73)	0.23^{aA} (0.11-0.46)	0.48^{bA} (0.06-0.58)
		T3	66.60^{bA} (55.86-81.54)	30.64^{aA} (0.80-34.99)	0.41^{bA} (0.19-0.66)	0.21^{aA} (0.05-0.44)

PS, Primescan; T3, TRIOS 3. Different superscript lowercase letters in each column indicate significant differences between scanners for each model-scanned area pair. Different superscript uppercase letters indicate significant differences between scanned areas for each model-scanner pair ($P<.05$).

each scanner-scanned area pair, while Figure 5 shows the box-plot graph of the precision of the measured deviations.

Table 3 summarizes the descriptive statistics of scan durations in each model for each scanner-scanned area pair. Significant differences were observed between scanners in each model ($P<.001$), as PS had lower scan duration than T3, regardless of the model and scanned area ($P\leq.010$). When the scanned area was considered, significant differences were observed in the posterior

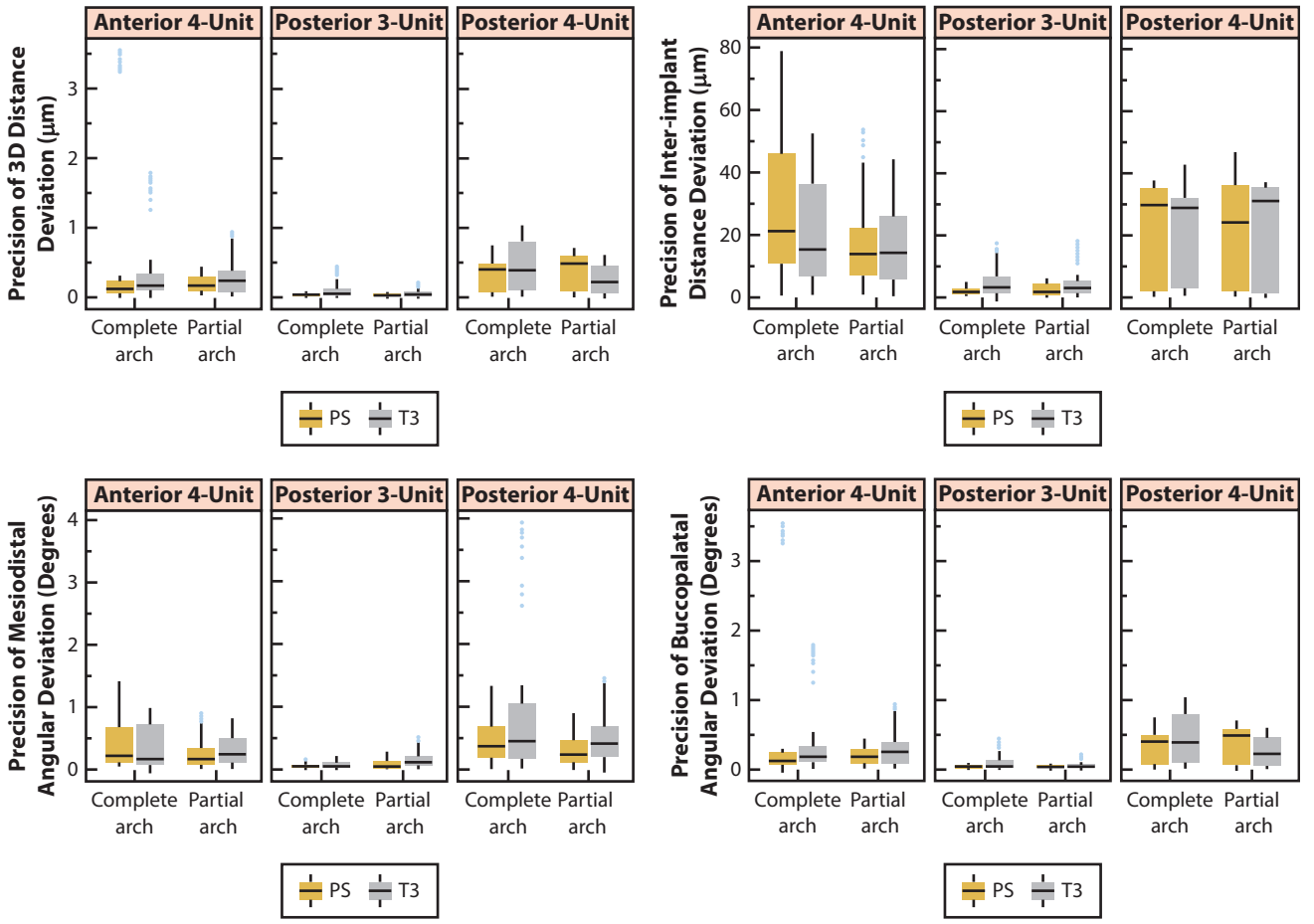

Figure 5. Box-plot graphs of precision of measured deviations for each scanner-scanned area pair in each model. PS, Primescan; T3, TRIOS 3.

3-unit and posterior 4-unit models ($P \leq .05$). Partial-arch scans led to lower scan duration for PS in both models ($P \leq .04$) and for T3 in the posterior 3-unit model ($P = .05$) (Fig. 6).

DISCUSSION

IOSs and scan areas affected the scan trueness and precision of implants placed to support an FPD. For time efficiency, PS required less time to make and process the scan, while partial-arch scans required less time when the posterior 3-unit and posterior 4-unit models were considered. Therefore, the null hypotheses were rejected.

When trueness and precision of the scanners were evaluated in each model, PS had outcomes either similar to or better than those for T3. When 3D distance deviations were considered, PS had higher accuracy in the anterior 4-unit and posterior 3-unit models and higher precision in the posterior 4-unit model. When interimplant distance deviations were considered, IOSs mostly had similar accuracy, with only PS having higher accuracy when complete-arch scans were performed on the posterior 3-unit model. When mesiodistal angular deviations were considered, PS had higher accuracy in the posterior 3-unit model and higher precision in the posterior 4-unit model. T3 had higher precision than PS only when buccopalatal angular deviations of the partial-arch scans of the posterior 4-unit model were considered.

Table 3. Median and interquartile range (25% to 75%) values of duration of scans for each scanner-scanned area pair within each model

Model	Scanned Area	Scanner	Scan Duration (s)
Anterior 4-unit	Complete arch	PS	261.71^{aA} (246.38-294.7)
		T3	363.24^{bA} (330.91-442.28)
	Partial arch	PS	230.88^{aA} (205.79-284.06)
		T3	342.6^{bA} (309.11-376.98)
Posterior 3-unit	Complete arch	PS	283.86^{aB} (247.26-316.56)
		T3	412.43^{bB} (363.93-454.99)
	Partial arch	PS	224.35^{aA} (187.88-250.9)
		T3	346.19^{bA} (305.22-406.08)
Posterior 4-unit	Complete arch	PS	270.68^{aB} (228.85-308.77)
		T3	418.38^{bA} (400.51-448.82)
	Partial arch	PS	205.1^{aA} (187.51-233.99)
		T3	388^{bA} (343.74-461.14)

PS, Primescan; T3, TRIOS 3. Different superscript lowercase letters in each column indicate significant differences between scanners for each model-scanned area pair. Different superscript uppercase letters indicate significant differences between scanned areas for each model-scanner pair ($P < .05$).

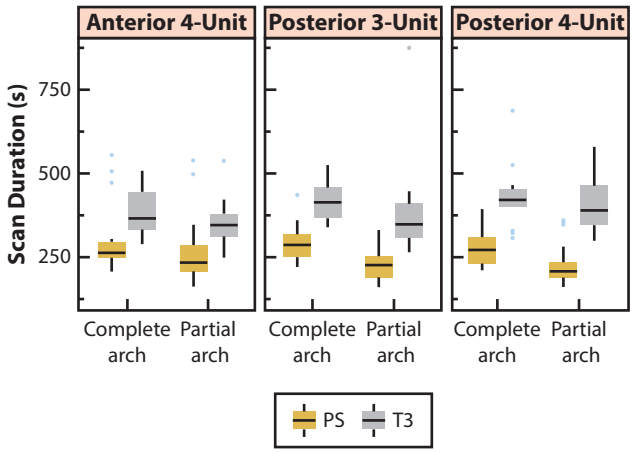

Figure 6. Box-plot graphs of scan durations for each scanner-scanned area pair in each model. PS, Primescan; T3, TRIOS 3.

Considering that the same operator performed each scan according to manufacturers' recommendations in the same standardized room, this difference between tested IOSs may be because they operated on different image-acquisition mechanisms; PS uses a smart pixel sensor, while T3 uses confocal microscopy and ultrafast optical scanning technology.[19]

Previous studies on scan accuracy of implant-supported FPDs digitized by using IOSs reported smaller deviations than the present study.[3,13,16,30-32] However, those studies had methodological differences with the present study. Results of previous studies on the scan accuracy of single implants, which used IOSs similar to those in the present study,[2,4,19-21] corroborate this hypothesis, as mean 3D distance deviations ranging from 35 μm[21] to 178 μm[20] have been reported. In the present study, median 3D distance deviations ranged between 8.75 μm and 172.17 μm, while median interimplant distance deviations ranged between 1.27 μm and 24.94 μm. Even though a consensus has not been reached regarding clinically acceptable misfit for implant-supported prostheses, a recent systematic review[37] reported that 160 μm of vertical and 150 μm of horizontal misfit did not lead to complications in implant-supported restorations. Another previous study[18] reported an interimplant distance deviation threshold of 100 μm and an angular deviation threshold of 0.4 degrees while digitizing 2 adjacent implants. Therefore, FPDs fabricated with the tested scans should have a clinically acceptable fit, particularly for the posterior 3-unit model. For the anterior 4-unit model, all IOS-scanned area pairs had median 3D distance deviations that were higher than those of other models and reported values, which may be associated with the curvature of the maxillary arch.[5] Angular deviation values in the posterior 4-unit model also support this hypothesis, as only unacceptable angular deviations were observed in this model. Even though this model had a posterior 4-unit edentulous area, 1 of the implants was placed at the canine site, the transition between the anterior and posterior arch.

Partial-arch scans mostly had trueness and precision similar to or better than those of complete-arch scans. Favorable results of partial-arch scans were most prominent when 3D distance deviations were considered, as, regardless of the IOS, partial-arch scans had higher accuracy in the posterior 3-unit model. This result could be associated with the anatomy of the posterior 3-unit model, as it was the only model with a 3-unit edentulous area and could be considered as the most straightforward situation among those tested. Even though no statistical analysis was performed among the tested models, the posterior 3-unit model had lower 3D distance deviations (trueness and precision) than the other models. This finding was consistent with that of previous studies,[16,25,26] which reported greater deviations with larger edentulous areas.

Regardless of the model and scanned area, PS had higher time efficiency than T3. Even though there are studies based on the time efficiency of IOSs,[7,13,17] the authors are unaware of a study using the same methodology while evaluating the time efficiency of the tested IOSs; thus, a comparison with previous studies was not possible. Nevertheless, a recent study[17] compared the scan duration of PS and T3 under different light conditions and concluded that PS required less time to complete a scan. However, the results of the present study cannot be generalized, as results may differ in situations where the STL file does not need to be transferred from an IOS to a CAD software program.

Partial-arch scans had higher time efficiency in the posterior 3-unit and posterior 4-unit models. Even for those situations when no significant difference between partial- and complete-arch scans was observed, partial-arch scans required less time for making and processing the scan. These results can be associated with the fact that fewer data were processed and stitched during partial-arch scans. Because the tested models represent different commonly encountered partially edentulous situations and PS and partial-arch scans generally had better results than their counterparts, clinicians may prefer partial-arch scans with PS to digitize implants placed for FPDs while working with the tested workflow. However, this hypothesis needs additional consideration, as parameters such as the initial investment and annual maintenance costs of an IOS also affect a clinician's decision.

Limitations of the in vitro study included that the scans were performed in controlled conditions[36] on a phantom head with an opposing jaw. However, patient-related factors could not be fully simulated.[19] Only 2 IOSs were evaluated. These had been reported to have high accuracy,[10,13] but different IOSs may affect the

results. Even though scanned metal models have favorable dimensional stability,[34] a scan spray had to be used to facilitate the scans of the reflective surfaces.[22] The authors consider the effect of layer thickness may be negligible given the fact that the model surfaces were not contacted until all scans were performed. Nevertheless, the presence or absence of the scan spray, particularly depending on the material being scanned, may affect the results. In addition, all partially edentulous models tested in the present study had 2 parallel implants. However, implant angulation[24] or the number of the implants[3] may affect the accuracy of a digital scan. The methodology used in the present study to evaluate deviations (RMS method, metrology-grade 3D analysis software program, and global best-fit algorithm) has been previously reported.[38] However, different deviation measurement methods,[39] or even the software program algorithm for 3D analysis to calculate RMS,[40] may also lead to different results. A previous study on the effect of the scanned area on measured deviations of a single anterior implant scan in a dentate arch reported that partial-arch scans resulted in higher trueness than complete-arch scans.[1] Considering the results of the present study and those of the study by Marques et al,[1] it can be speculated that partial-arch scans of tested FPD situations would not only lead to more accurate prostheses but also require fewer adjustments with less distortion of the remaining arch. Nevertheless, future in vivo studies on the fit and adjustments of FPDs fabricated with the scans of tested IOSs in different partially edentulous situations are needed to corroborate the findings of this study.

CONCLUSIONS

Based on the findings of this in vitro study, the following conclusions were drawn:

1. PS had mostly higher 3D trueness, and partial-arch scans with both IOSs had higher 3D trueness with the posterior model for the 4-unit FPD. The tested scanners and scan area mostly did not affect the interimplant distance and angular deviations of the scans.
2. Partial-arch scans with PS in 4-unit FPD models had higher precision when 3D distance deviations were considered. The tested scanners and scan area mostly did not affect the scan precision when interimplant distance and angular deviations were considered.
3. PS had higher time efficiency than T3 regardless of the model and scanned area tested. Partial-arch scans had higher time efficiency when the posterior 4-unit edentulous area model was considered. The partial-arch scans also had higher time efficiency when PS was used to digitize the 3-unit edentulous area model.

REFERENCES

1. Marques VR, Çakmak G, Yilmaz H, Abou-Ayash S, Donmez MB, Yilmaz B. Effect of scanned area and operator on the accuracy of dentate arch scans with a single implant. *J Clin Med*. 2022;11:4125.
2. Yilmaz H, Arınç H, Çakmak G, et al. Effect of scan pattern on the scan accuracy of a combined healing abutment scan body system. *J Prosthet Dent*. 23 Febuary 2022. https://doi.org/10.1016/j.prosdent.2022.01.018 [Epub ahead of print.].
3. Mangano FG, Hauschild U, Veronesi G, Imburgia M, Mangano C, Admakin O. Trueness and precision of 5 intraoral scanners in the impressions of single and multiple implants: a comparative in vitro study. *BMC Oral Health*. 2019;19:101.
4. Donmez MB, Çakmak G, Atalay S, Yilmaz H, Yilmaz B. Trueness and precision of combined healing abutment-scan body system depending on the scan pattern and implant location: an in-vitro study. *J Dent*. 2022;124:104169.
5. Mizumoto RM, Alp G, Özcan M, Yilmaz B. The effect of scanning the palate and scan body position on the accuracy of complete-arch implant scans. *Clin Implant Dent Relat Res*. 2019;21:987–994.
6. Mangano F, Lerner H, Margiani B, Solop I, Latuta N, Admakin O. Congruence between meshes and library files of implant scanbodies: an in vitro study comparing five intraoral scanners. *J Clin Med*. 2020;9:2174.
7. Siqueira R, Galli M, Chen Z, et al. Intraoral scanning reduces procedure time and improves patient comfort in fixed prosthodontics and implant dentistry: a systematic review. *Clin Oral Investig*. 2021;25:6517–6531.
8. Donmez MB, Marques VR, Çakmak G, Yilmaz H, Schimmel M, Yilmaz B. Congruence between the meshes of a combined healing abutment-scan body system acquired with four different intraoral scanners and the corresponding library file: an in vitro analysis. *J Dent*. 2022;118:103938.
9. Joda T, Lenherr P, Dedem P, Kovaltschuk I, Bragger U, Zitzmann NU. Time efficiency, difficulty, and operator's preference comparing digital and conventional implant impressions: a randomized controlled trial. *Clin Oral Implants Res*. 2017;28:1318–1323.
10. Róth I, Czigola A, Fehér D, et al. Digital intraoral scanner devices: a validation study based on common evaluation criteria. *BMC Oral Health*. 2022;22:140.
11. Waldecker M, Rues S, Awounvo Awounvo JS, Rammelsberg P, Bömicke W. In vitro accuracy of digital and conventional impressions in the partially edentulous maxilla. *Clin Oral Investig*. 2022;26:6491–6502.
12. Ender A, Zimmermann M, Mehl A. Accuracy of complete- and partial-arch impressions of actual intraoral scanning systems in vitro. *Int J Comput Dent*. 2019;22:11–19.
13. Imburgia M, Logozzo S, Hauschild U, Veronesi G, Mangano C, Mangano FG. Accuracy of four intraoral scanners in oral implantology: a comparative in vitro study. *BMC Oral Health*. 2017;17:92.
14. Abduo J, Elseyoufi M. Accuracy of Intraoral Scanners: a systematic review of influencing factors. *Eur J Prosthodont Restor Dent*. 2018;26:101–121.
15. Flügge T, van der Meer WJ, Gonzalez BG, Vach K, Wismeijer D, Wang P. The accuracy of different dental impression techniques for implant-supported dental prostheses: a systematic review and meta-analysis. *Clin Oral Implants Res*. 2018;29(Suppl 16):374–392.
16. Thanasrisuebwong P, Kulchotirat T, Anunmana C. Effects of inter-implant distance on the accuracy of intraoral scanner: an in vitro study. *J Adv Prosthodont*. 2021;13:107–116.
17. Ochoa-López G, Cascos R, Antonaya-Martín JL, Revilla-León M, Gómez-Polo M. Influence of ambient light conditions on the accuracy and scanning time of seven intraoral scanners in complete-arch implant scans. *J Dent*. 2022;121:104138.
18. Andriessen FS, Rijkens DR, van der Meer WJ, Wismeijer DW. Applicability and accuracy of an intraoral scanner for scanning multiple implants in edentulous mandibles: a pilot study. *J Prosthet Dent*. 2014;111:186–194.
19. Çakmak G, Donmez MB, Atalay S, Yilmaz H, Kökat AM, Yilmaz B. Accuracy of single implant scans with a combined healing abutment-scan body system and different intraoral scanners: an in vitro study. *J Dent*. 2021;113:103773.
20. Yilmaz B, Gouveia D, Marques VR, Diker E, Schimmel M, Abou-Ayash S. The accuracy of single implant scans with a healing abutment-scanpeg system compared with the scans of a scanbody and conventional impressions: an in vitro study. *J Dent*. 2021;110:103684.
21. Atalay S, Çakmak G, Donmez MB, Yilmaz H, Kökat AM, Yilmaz B. Effect of implant location and operator on the accuracy of implant scans using a combined healing abutment-scan body system. *J Dent*. 2021;115:103855.
22. Oh HS, Lim YJ, Kim B, Kim MJ, Kwon HB, Baek YW. Influence of scanning-aid materials on the accuracy and time efficiency of intraoral scanners for full-arch digital scanning: an in vitro study. *Materials (Basel)*. 2021;14:2340.
23. Sanda M, Miyoshi K, Baba K. Trueness and precision of digital implant impressions by intraoral scanners: a literature review. *Int J Implant Dent*. 2021;7:97.
24. Arora A, Upadhyaya V, Parashar KR, Malik D. Evaluation of the effect of implant angulations and impression techniques on implant cast accuracy - An in vitro study. *J Indian Prosthodont Soc*. 2019;19:149–158.
25. Fattouh M, Kenawi LMM, Fattouh H. Effect of posterior span length on the trueness and precision of 3 intraoral digital scanners: a comparative 3-dimensional in vitro study. *Imaging Sci Dent*. 2021;51:399–406.

26. Vandeweghe S, Vervack V, Dierens M, De Bruyn H. Accuracy of digital impressions of multiple dental implants: an in vitro study. *Clin Oral Implants Res*. 2017;28:648–653.
27. Chen Y, Zhai Z, Watanabe S, Nakano T, Ishigaki S. Understanding the effect of scan spans on the accuracy of intraoral and desktop scanners. *J Dent*. 2022;124:104220.
28. Son K, Lee KB. Effect of tooth types on the accuracy of dental 3D scanners: an in vitro study. *Materials (Basel)*. 2020;13:1744.
29. Moon YG, Lee KM. Comparison of the accuracy of intraoral scans between complete-arch scan and quadrant scan. *Prog Orthod*. 2020;21:36.
30. Canullo L, Colombo M, Menini M, Sorge P, Pesce P. Trueness of intraoral scanners considering operator experience and three different implant scenarios: a preliminary report. *Int J Prosthodont*. 2021;34:250–253.
31. Fukazawa S, Odaira C, Kondo H. Investigation of accuracy and reproducibility of abutment position by intraoral scanners. *J Prosthodont Res*. 2017;61:450–459.
32. Pesce P, Bagnasco F, Pancini N, et al. Trueness of intraoral scanners in implant-supported rehabilitations: an in vitro analysis on the effect of operators' experience and implant number. *J Clin Med*. 2021;10:5917.
33. Abou-Ayash S, Mathey A, Gäumann F, Mathey A, Donmez MB, Yilmaz B. In vitro scan accuracy and time efficiency in various implant-supported fixed partial denture situations. *J Dent*. 2022;127:104358.
34. Hamm J, Berndt EU, Beuer F, Zachriat C. Evaluation of model materials for CAD/CAM in vitro studies. *Int J Comput Dent*. 2020;23:49–56.
35. Rödiger M, Heinitz A, Bürgers R, Rinke S. Fitting accuracy of zirconia single crowns produced via digital and conventional impressions-a clinical comparative study. *Clin Oral Investig*. 2017;21:579–587.
36. Revilla-León M, Subramanian SG, Att W, Krishnamurthy VR. Analysis of different illuminance of the room lighting condition on the accuracy (trueness and precision) of an intraoral scanner. *J Prosthodont*. 2021;30:157–162.
37. Abdelrehim A, Etajuri EA, Sulaiman E, Sofian H, Salleh NM. Magnitude of misfit threshold in implant-supported restorations: a systematic review. *J Prosthet Dent*. 7 November 2022. https://doi.org/10.1016/j.prosdent.2022.09.010 [Epub ahead of print.].
38. Yilmaz B, Marques VR, Donmez MB, et al. Influence of 3D analysis software on measured deviations of CAD-CAM resin crowns from virtual design file: an in-vitro study. *J Dent*. 2022;118:103933.
39. Lerner H, Nagy K, Pranno N, Zarone F, Admakin O, Mangano F. Trueness and precision of 3D-printed versus milled monolithic zirconia crowns: an in vitro study. *J Dent*. 2021;113:103792.
40. Son K, Lee WS, Lee KB. Effect of different software programs on the accuracy of dental scanner using three-dimensional analysis. *Int J Environ Res Public Health*. 2021;18:8449.

Corresponding author:
Dr Mustafa Borga Dönmez
Department of Reconstructive Dentistry and Gerodontology
School of Dental Medicine
University of Bern
7 Freiburgstrasse
Bern 3007
SWITZERLAND
Email: mustafa-borga.doenmez@unibe.ch

CRediT authorship contribution statement

Mustafa Borga Donmez: Writing – original draft, preparation. **Ayse Mathey:** Conceptualization, Methodology, Investigation. **Fabio Gäumann:** Methodology, Investigation. **Amber Mathey:** Methodology, Investigation. **Burak Yilmaz:** Supervision, Writing – review & editing. **Samir Abou-Ayash:** Conceptualization, Data curation, Formal analysis, Funding acquisition, Project administration.

https://doi.org/10.1016/j.prosdent.2023.01.029